

# Chapter 4

## The Experimental Apparatus: A One Degree-of-Freedom Manipulandum

### 4.1 Mechanical and Computer Hardware

The apparatus used to conduct the experiments was a one degree-of-freedom manipulandum (or haptic display), shown in Figure 4.1. The system comprised a crank attached directly to the output shaft of a DC motor, an optical encoder, a fluid-filled mechanical damper, and a PC-based digital controller. A schematic of the manipulandum is shown in Figure 4.2. The lever arm attached to the motor shaft was 15.24 cm (6 inches) in length. The handle was mounted on rotary bearings so that it was free to rotate about its own axis. The lever arm was rigidly connected to the motor shaft by a 3/4 inch diameter steel drive shaft (i.e. the device was direct drive). The drive shaft was supported on two bearings, one above and one below the mechanical damper, which was mounted in line with the drive shaft (see Figure 4.2). The motor, support bearings, and damper housing were all supported by a box-like structure made of aluminum plate. The box was in turn rigidly attached to a heavy aluminum table. In Figure 4.1 the motor and damper cannot be seen, as the motor extends below the surface of the table, and the damper is fully enclosed in the box. The components of the mechanism will now be described in detail.



Figure 4.1 One degree-of-freedom manipulandum used in experiments. Experimental setup with CRT display and subject grasping handle. In Experiment I, a shroud (not shown) prevented subjects from seeing their hand or the handle.

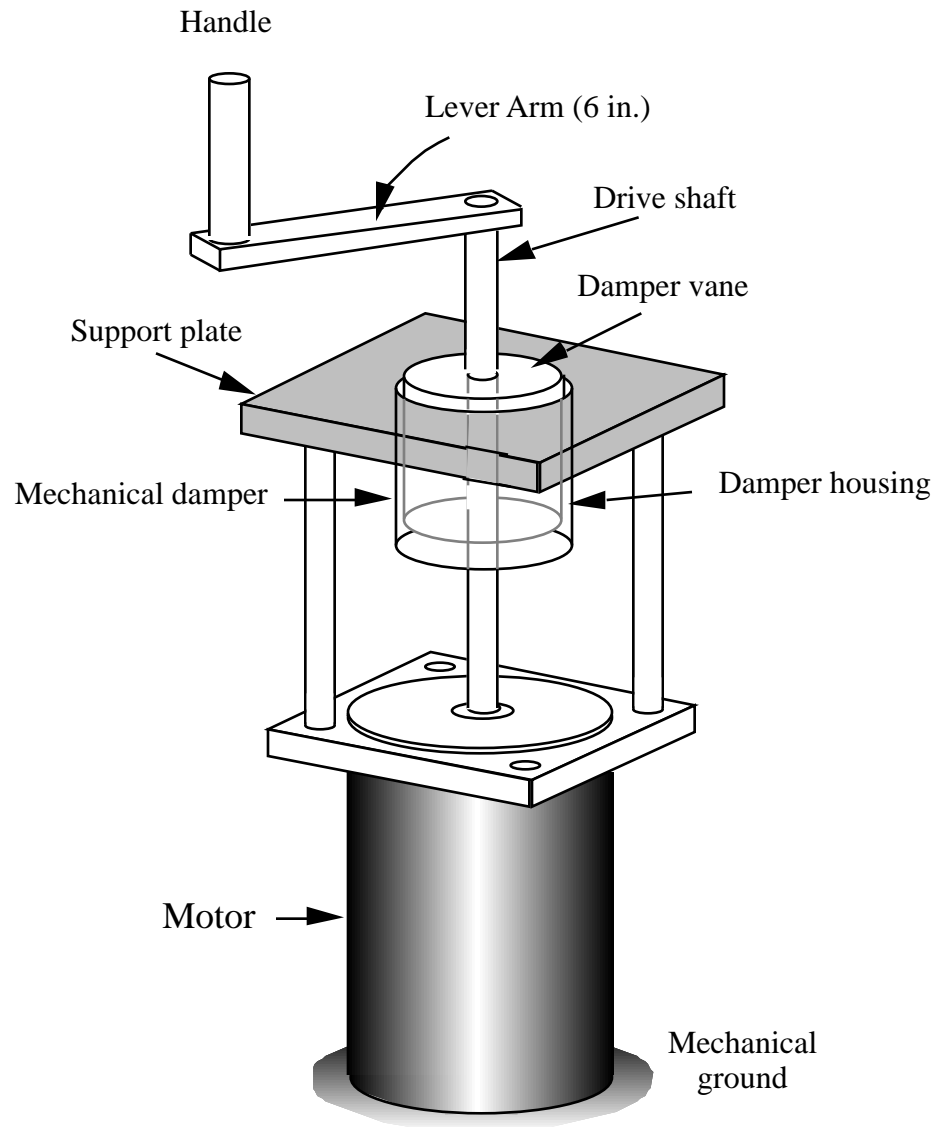


Figure 4.2. Sketch of one degree-of freedom "crank" manipulandum featuring direct drive and a fluid-filled mechanical damper. The motor and damper housing were fixed to mechanical ground. The damper vane rotated with the drive shaft.

#### *4.1.1 Motor and Amplifier*

Mechanical actuation was supplied by a DC brushless motor (Electro-Craft model S-4075) driven by a pulse-width-modulated servo amplifier (Electro-Craft model DM30). The motor was capable of generating peak torques of 20 N·m and continuous stall torques of 10 N·m, which correspond to handle forces of 130 N and 65 N respectively. The rotor inertia was  $6.8 \times 10^{-3} \text{ kg}\cdot\text{m}^2$ , or 0.03 kg as seen from the handle.

The switching frequency of the pulse-width modulated motor amplifier was 10 kHz. It was used in a torque control mode, so that the amplifier current (and presumably the motor torque) was proportional to a command voltage from the computer controller.

#### *4.1.2 The Physical Damper and Damping Cancellation*

A mechanical damper was added to the mechanism to improve the stability properties of the device under feedback control, particularly for higher impedance environment simulations (Colgate and Brown, 1994, Colgate and Schenkel, 1994). Without the damper, some of the higher levels of stiffness and damping that were simulated in the experiments would not have been stable, i.e. they would have caused uncontrolled oscillations of the handle under certain conditions. The damper helped prevent limit cycling behavior (oscillations) by dissipating energy. The drawback of adding a damper was that it made the device less backdriveable. To minimize this effect, the torque generated by the damper was measured, then digitally filtered with a 4-pole modified Butterworth lowpass filter ( $f_c = 10 \text{ Hz}$ ), and subtracted from the motor torque command. The torque feedback made the device backdriveable at low frequencies, however since the damping torque feedback signal was attenuated at higher frequencies, the damping was not cancelled in that frequency range. This was important, because the frequencies of the limit cycles are, in general, greater than the bandwidth of voluntary motion. The net effect was improved stability without significantly compromising backdriveability.

The damper was constructed as shown in Figure 4.3. A cylindrical vane, rigidly attached to the drive shaft, moved inside a hollow annular region formed in a stationary housing (cup). A very viscous silicone fluid (30,000 centistokes) filled the space between the moving vane and the stationary cup. The shearing of the fluid in the narrow gaps (0.045 in.) between the surfaces of the vane and cup generated a damping torque on the drive shaft. The torque vs. velocity characteristic of the damper was non-linear (torque varied as approx. the square-root of velocity) and time varying. The fluid-filled damper generated roughly 40 N·s/m of damping. Note that the damper design required no seals, so it was frictionless.

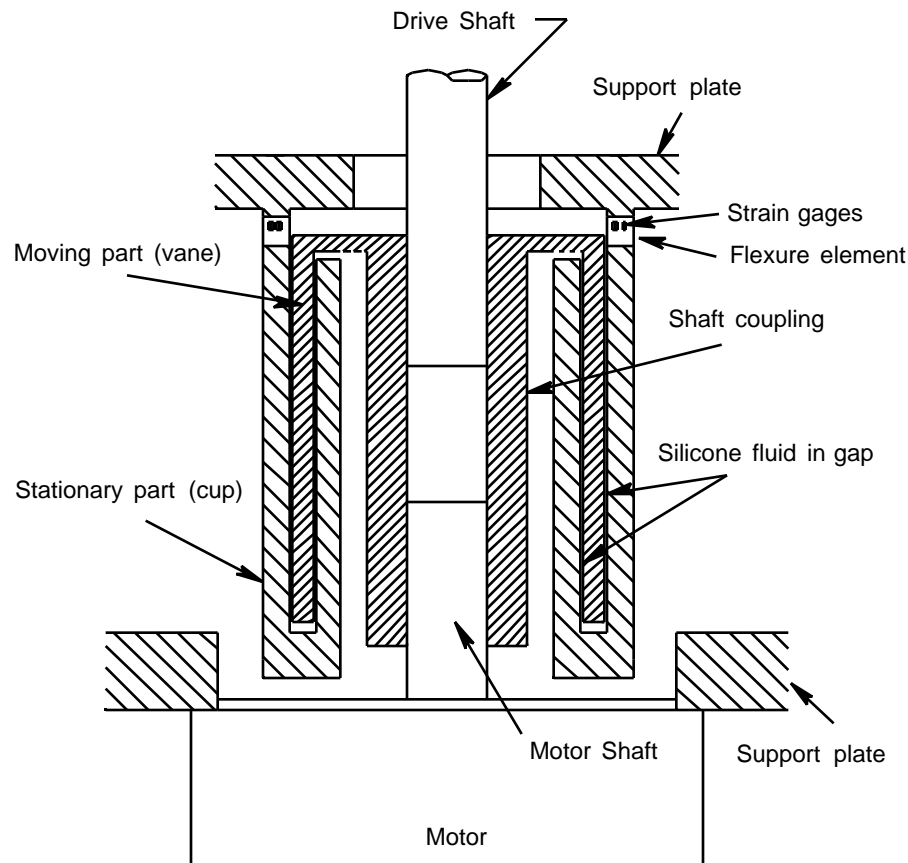


Figure 4.3 Cross-section of fluid-filled mechanical damper. A cylindrical vane which was rigidly attached to the drive shaft moved inside a cup which was attached to the mechanism housing. Viscous silicone fluid in the gaps between the vane and cup surfaces created drag.

The damping torque was equal to the reaction torque of the damper housing against mechanical ground. This reaction torque was measured by mounting strain gages (Entran semiconductor strain gages, model ESU-060-500) on thin flexure elements that were machined into the damper housing. The torque signal was lowpass filtered in the digital controller.

The mechanical damping and torque feedback parameters remained constant throughout the two experiments, and had no relation to the software-controlled (virtual) damping parameters that were varied in the experiments.

#### *4.1.3 Optical Encoder*

A rotary optical incremental encoder (Gurley Precision Instruments, model 8335-25) was mounted on the motor shaft, at the end opposite the drive shaft and damper. The encoder had a line count of 11,250. A high resolution interpolator electronics module (Gurley Precision Instruments, model HR-20) increased the resolution of the encoder by a factor of 80 (20× by interpolation and 4× by quadrature), resulting in 900,000 counts per revolution. The resulting position resolution at the handle was 1.1 μm.

#### *4.1.4 Computer and Interface Boards*

Two different PC-compatible computers were used to control the manipulandum. In Experiment I, a 50 MHz, 486 IBM AT-compatible computer was used, and in Experiment II a 90 MHz Pentium computer was used. Both machines were more than fast enough to compute the control algorithms and generate the graphical displays for the experiments.

A PC-compatible encoder card (Technology 80 Inc., model 5312B) provided the interface between the encoder and the computer. A 16-bit A/D channel for the damping torque signal and a 12-bit D/A channel for the motor torque command signal were provided by an analog I/O board (Computer Boards Inc., model CIO-DAS1602/16)

## 4.2 Digital Controller

Damping cancellation and virtual environment simulations were implemented in a digital control algorithm running on the PC. The algorithms were written in the C programming language. The digital controller was executed as an interrupt-service routine, which was triggered at precise intervals by a clock on the A/D board. Whenever the control algorithm was not being executed, the processor was free to execute the graphics and keyboard input/output code. Controller update rates were 1000 Hz for Experiment I and 3000 Hz for Experiment II. The time required to execute the control algorithm for each experiment was just under 0.1 milliseconds (as tested on the Pentium).

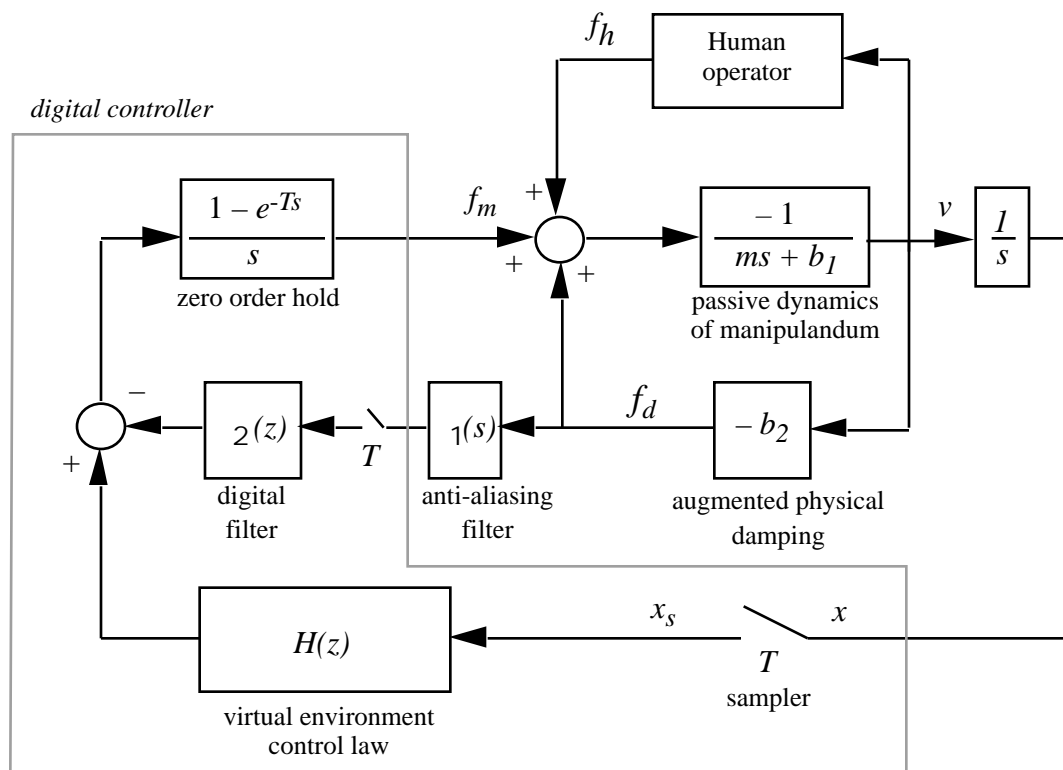


Figure 4.4 Block diagram of manipulum, controller, and human operator. The force generated by the physical damper is sampled and digitally filtered in the controller. The virtual environment simulation is also computed in the digital controller.

A block diagram of the manipulandum, human operator, digital controller, and I/O hardware is presented in Figure 4.4. In each sampling period, the controller received as inputs the position of the handle (from the optical encoder) and the damping torque (from the strain gage sensor). The digital controller estimated handle velocity from the position signal in one of two ways. In Experiment I, velocity was estimated using a first-order recursive differentiator plus a lowpass filter, with the cutoff frequency set at 8 Hz. In Experiment II, a second-order low-pass filter with a cutoff frequency of 30 Hz was used. Both exhibited similar stability properties, but the second order filter with a higher cutoff frequency caused less phase shift at low frequencies (approaching the bandwidth of human voluntary motion).

The controller then computed a desired handle force based on handle position and/or velocity. The controller also digitally filtered the damping torque signal and subtracted it from the desired handle force. The result was output through the D/A to the motor amplifier. Handle force was not measured (except for data collection purposes), nor was it fed back to the controller. Because of the low inertia and friction of the device, this open-loop control scheme worked well, and avoided complications and potential instability problems associated with force regulation.

In the remainder of this chapter, the question of how well the device generated the desired handle forces will be examined, and the overall performance of the device will be characterized.

### 4.3 Performance Measures

In this section, three main performance measures will be discussed: isometric force bandwidth, vibratory noise power spectrum, and handle impedance under real-time control. A torque sensor was added to the manipulandum to collect the necessary data. The torque

sensor was mounted between the top of the drive shaft and the lever arm. At this location the only impedance between the torque sensor and the person's hand was the mass of the handle and lever arm. The torque sensor was actually a 6-axis force/torque sensor (Assurance Technologies Inc., model 15/50), but only the z-axis torque was used. The resolution of the sensor, converted to handle coordinates, was 0.02 N. The precise bandwidth of the torque sensor is not known, although it is estimated to extend to approximately 200 Hz (see Section 4.3.2). The form of the output from the sensor was an analog voltage. From force and accelerometer data recorded while lightly tapping the lever arm of the manipulandum with a hammer, a delay of approximately 3 ms in the force sensor response was measured. The semiconductor strain gage accelerometer (Entran model EGE-72B-200,  $\pm 200$  g, 0–1000 Hz) was mounted to the end of the lever arm of the manipulandum, just below the handle. A pure delay is expected in the analog output of the force sensor because the strain gage signals are digitally sampled, processed, and reconverted to analog voltages by a controller module (ATI controller, model 15/50).

A digital oscilloscope with a floppy drive storage device was used to collect all torque sensor data. The oscilloscope was used instead of the spare channels of the A/D board because of severe noise/grounding problems encountered when the additional sensor and power supply electronics were connected to the existing control circuit. The source of the noise was presumably the PWM motor amplifier.

#### *4.3.1 Isometric Force Bandwidth*

The transfer function from commanded force to the actual isometric force generated by the motor was measured from 5 Hz to 100 Hz, at 5 Hz intervals. The magnitude of the transfer function is plotted vs. frequency in Figure 4.5. The force generated by the motor was measured by removing the manipulandum lever arm and handle, attaching one end of

the torque sensor to the top of the drive shaft, and fixing the other end of the sensor to mechanical ground. A sinusoidal torque command was generated by the controller, and the resulting output torque was recorded for one second at a 1000 Hz sampling frequency. The amplitude of the commanded force was 6.5 N. The transfer function was computed using Matlab's™ *tfe* function. The algorithm computes the transfer function as the quotient of the cross spectrum of input (x) and output (y), and the power spectrum of the input:

$$T_{xy}(f) = \frac{P_{xy}(f)}{P_{xx}(f)} \quad (4.1)$$

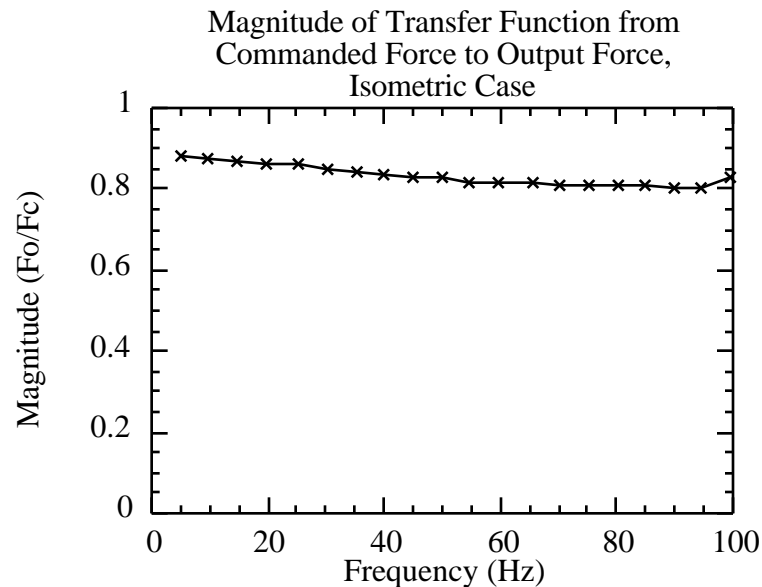


Figure 4.5 Magnitude of the transfer function from commanded force to isometric output force between 5 Hz and 100 Hz.

In the frequency range tested, the magnitude of the output force was 80-88% of the nominal force command, with the maximum occurring at 5 Hz, and the minimum occurring at 90 Hz. These results indicate that the motor and amplifier have a reasonably constant force output across the frequency range of interest.

The transfer function from commanded force to output force (again isometric) was also measured at 0 Hz. Force amplitudes between -10 N and +10 N, at 2 N intervals, were tested. Output force is plotted vs. commanded force in Figure 4.6. The ratio of output force to commanded force was between 0.79 and 0.92 (excluding the 0 N case). The ratio increased with force amplitude. Poorer performance at low force levels is probably due to friction in the motor and manipulandum bearings. Performance only began to drop off at 2 N, which is 3% of the motor's maximum stall force, and 1.5% of its peak force.

To summarize, the isometric force measurements showed that the transfer function from commanded force to output force was relatively constant from zero to 100 Hz, as long as the force command was not very small.

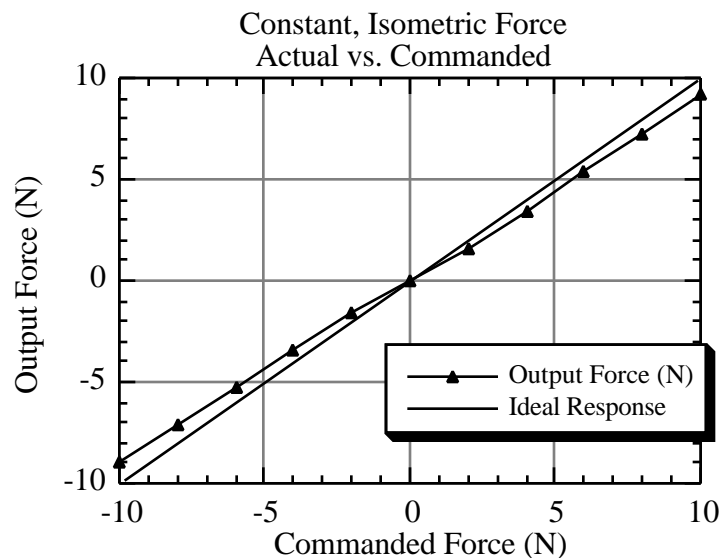


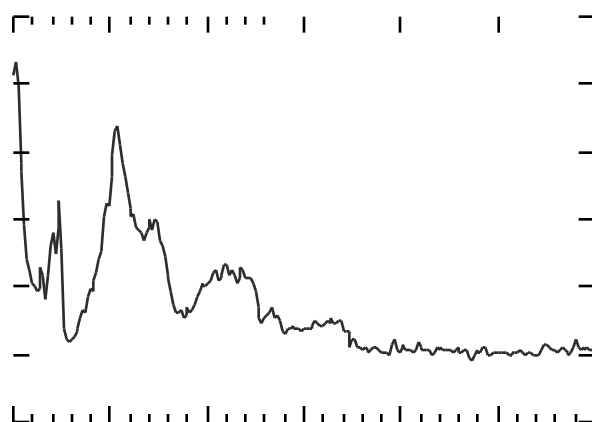
Figure 4.6 Average isometric force output vs. amplitude of DC force command. Straight line is ideal (unity gain) response.

#### 4.3.2 Mechanical Noise

When the PWM amplifier was "enabled" (i.e. it was sending current to the motor coils), the motor generated faint high frequency sounds and a perceptible vibration at the handle. The origin of the vibrations was apparently electrical noise on the torque command signal to the amplifier, generated by the PWM amplifier. Concerted efforts to reduce this noise by shielding and proper grounding resulted in the noise levels described.

Two types of data were collected to quantify the motor noise: displacement with the handle unconstrained, and force with the handle rigidly constrained. Measuring displacement had the advantage that it was not bandwidth limited, as was the force sensor. The force sensor, however, could be used to measure the noise at different levels of motor force output. The noise in the force and displacement signals was quantified using two measures: power spectra and RMS (standard deviation of the signal about its mean).

The power spectrum of the noise in the displacement signal is shown in Figure 4.7. The spectrum shown is the ensemble average of 10 motion records, each 4000 points long, sampled at 3000 Hz. The largest peaks are at 6 Hz, 120 Hz, and 275 Hz. A lesser contribution to the noise appears in the 500-600 Hz range. The 10 records were collected at different handle positions, spaced roughly 2 cm apart. The spectra of individual displacement records were generally quite similar, differing mainly in the size of the peak at 6 Hz and the location of the peak around 550 Hz. Three of the force records (for three different handle positions) are plotted vs. time in Figure 4.8. They represent the most extreme differences in amplitude and frequency content of the ten data sets recorded.



After subtracting the mean and linear trend from each displacement record, the RMS (standard deviation) of each was computed. RMS values ranged from 1.3–9.5  $\mu\text{m}$ , and the average of the ten records was 3.7  $\mu\text{m}$ .

The peak-to-peak amplitude of the 275 Hz vibrations was on the order of 5 to 10  $\mu\text{m}$ . From these measurements one can reasonably conclude that vibrations in this frequency range were perceptible to users. When a person grasped the handle, the amplitude of vibration certainly decreased, but probably not to less than the absolute threshold for detection ( $\sim 1\mu\text{m}$ ).

The noise in the motor output was also measured at different output force levels. To do this, the handle was rigidly constrained, and the output force was measured using the torque sensor. For different output force levels, the overall power, or standard deviation, of the noise did not vary greatly, but the spectrum of the noise did.

The same data that were used to construct Figure 4.6 (average force output) was used to characterize the variance in the force output (noise). The spectra of the noise in the output force is shown in Figures 4.9 and 4.10. Each spectrum corresponds to a different commanded force amplitude. The spectra are substantially different for the different force levels.

Another feature of the force spectra are that they roll off above 200 Hz. Moreover, the peaks at 275 Hz and 550 Hz which were observed in the displacement signals are not observed in the force signals. From both of these observations we can conclude that the bandwidth of the force sensor extended only to approximately 200 Hz.

Although the frequency content of the noise varied substantially with the average force level, the total energy, or magnitude of the noise did not. The RMS of the force noise is plotted vs. commanded force in Figure 4.11. The noise RMS ranged between 0.025 N and 0.055 N.

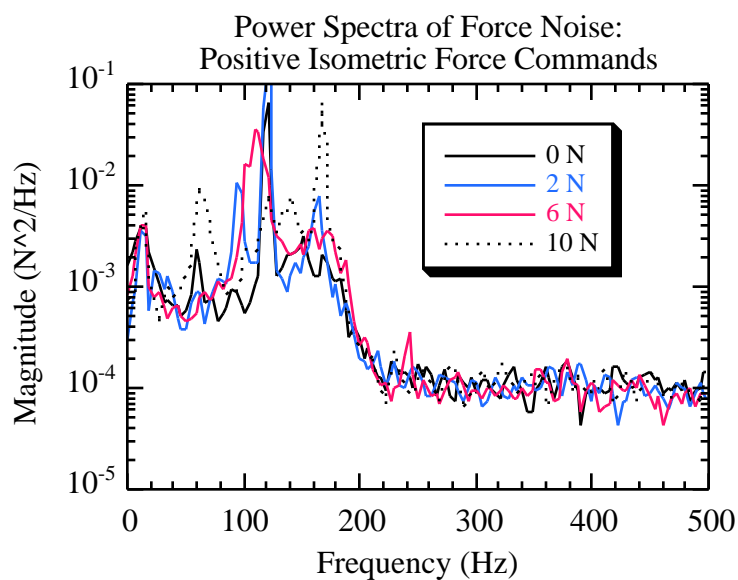


Figure 4.9 Power spectra of noise in force output. Different spectra correspond to different commanded force levels.

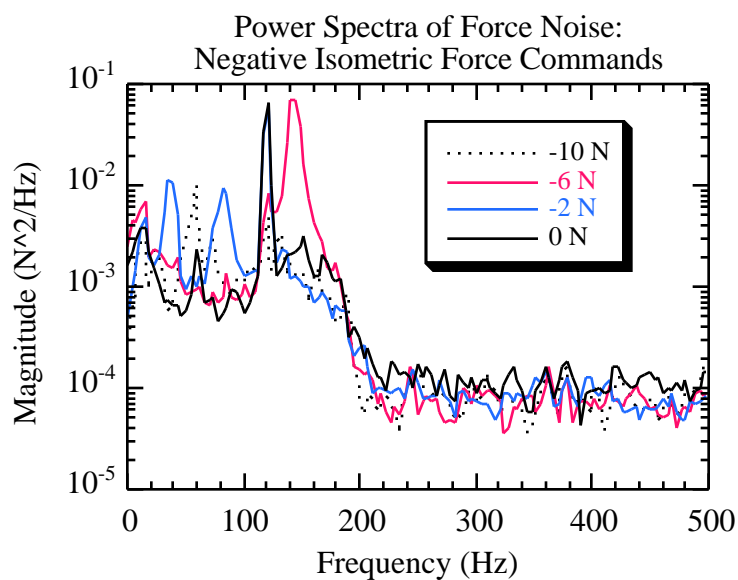


Figure 4.10 Power spectra of noise in force output. Different spectra correspond to different commanded force levels.

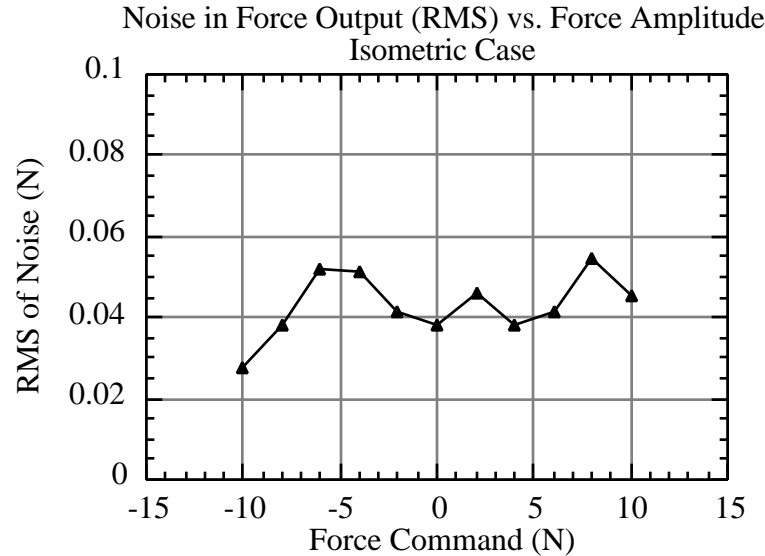


Figure 4.11 Magnitude of noise in force output vs. magnitude of commanded force.

Finally, handle force was also measured while the author moved the handle by hand. The power spectra of these data were not computed, but peak-to-peak amplitudes of the vibrations were estimated from the time domain records. They were typically between 0.05-0.10 N. These variations in force could have had a significant effect on the thresholds of feature detection that were measured in the experiments, as many of those features were characterized by rapid changes in force of less than 1.0 N. The issue of noise in the apparatus masking features that subjects were asked to detect is discussed further in Chapter 6, Section 6.5.

In summary, the energy of the vibrations was relatively independent of motor position and output torque. The frequency content of the noise was also relatively independent of position (at least at zero average force amplitude), but the frequency content changed substantially for different force amplitudes. The dependence of the noise on motor velocity is not known, however informal observations indicate that slow speeds are noisier than moderate to fast speeds.

### 4.3.3 Measured Handle Impedance

As another means of assessing the performance of the manipulandum, the endpoint impedance of the device was measured and compared to the nominal controller values. One can think of the manipulandum as an impedance display – a device controlled to exhibit a desired relationship between handle motion and handle force. When the impedance being simulated is zero (or null), an ideal haptic display should exhibit no mass, no damping, no stiffness, etc. Real haptic displays cannot achieve this ideal, but a low impedance is desirable. Also, when a larger impedance is desired, the handle impedance should closely match the desired value.

The impedance of the manipulandum was measured for two different environment simulations: zero nominal impedance, and 50 N·s/m of virtual damping. Measuring zero nominal impedance provided a measure of how well the torque feedback control loop was cancelling the physical damping at low frequencies. Position and force data for computing the handle impedance were collected while the author moved (shook) the handle back and forth at various amplitudes and frequencies of motion. Because of the limited bandwidth of voluntary motion, the transfer function is only valid at low frequencies (below 9 Hz). The data were collected using the controller parameters listed in Table 4.1.

Table 4.1  
Controller Parameters for Impedance Measurements

Controller update rate = 1000 Hz
Damping-torque feedback: Lowpass filter cutoff frequency = 10 Hz
Velocity estimator: Lowpass filter cutoff frequency = 30 Hz Filter order: 2

Another parameter was important in determining the backdriveability of the device – the gain in the torque-feedback loop. The total gain was equal to the gain of the strain gage amplifying circuit, plus a gain (constant multiplier) in the digital controller. The controller gain was adjusted to the greatest magnitude possible such that the handle slowed down on its own when it was released.

The complex transfer function from handle motion (as measured by the encoder) to handle force (as measured by the torque sensor) was computed using Equation 4.1 (Matlab's *tfe* function). Twenty force and position data records, each 4000 points long, were collected at a sampling rate of 200 Hz. The cross spectrum and the power spectrum were computed on the concatenated data. The mass and damping estimates were obtained from the transfer function according to Equation 4.2:

$$\frac{F(j)}{x(j)} = m(j)^2 + b(j) \quad (4.2)$$

where  $\frac{F(j)}{x(j)}$  is the complex value of the transfer function at frequency  $j$ ,  $m$  is mass and  $b$  is damping. Given the value of the transfer function, Equation 4.2 can be rearranged to solve for  $m$  and  $b$ .

$$m = -\frac{1}{2} \operatorname{Re} \frac{F(j)}{x(j)} \quad \text{and} \quad b = \frac{1}{2} \operatorname{Im} \frac{F(j)}{x(j)} \quad (4.3)$$

where  $\operatorname{Re} \frac{F(j)}{x(j)}$  is the real component of the transfer function at frequency  $j$ , and  $\operatorname{Im} \frac{F(j)}{x(j)}$  is the imaginary component.

The estimated mass and damping for the null environment case are plotted vs. frequency in Figures 4.8 and 4.9. The results were corrected for the 3 ms delay in the force signal. The estimates are only valid in the frequency range between 0.5 and 8.8 Hz. In this range, the coherence function between the two signals was greater than 0.9. Above 9 Hz, the coherence dropped sharply to near zero. Coherence is a measure of how well correlated two signals are. A coherence value near one indicates tight correlation, and a value of zero represents no correlation, or complete independence of two signals. Special effort was made to shake the handle at a variety of frequencies, including the highest frequencies possible, so that the transfer function would be accurate across a broad frequency range. A serendipitous result of the measurements of handle impedance was the measurement of the bandwidth of voluntary motion, approximately 0–8 Hz.

The damping estimate varied from 2 N·s/m at 0.5 Hz to approximately 8 N·s/m at 8 Hz. The maximum implementable (i.e. stable) virtual damping was 200 N·s/m, therefore, the minimum implementable damping was between 1% and 4% of maximum, within the range of voluntary motion. Moreover, the results of Experiment I will show that perception of features, as well as speed and accuracy of motions do not depend significantly on the level of uniform damping in the environment (see Section 5.xx). Therefore, the uncompensated damping of the handle is not believed to have affected the results of either Experiment I or Experiment II.

The estimated handle inertia for the null environment is shown in Figure 4.9. It is approximately 0.5 kg from 0.8 Hz. This inertia is the result, primarily, of phase lead in the torque feedback signal at low frequencies, caused by the lowpass torque filter. It does not include the mass of the handle and lever arm because they were distal to the torque sensor. The mass of the handle and lever arm were estimated by measuring each parts' mass and calculating its moment of inertia with respect to the axis of the drive shaft. The inertia of

the handle and lever arm was approximately 0.35 kg, making the total inertia of the device under real-time control approximately 0.85 kg.

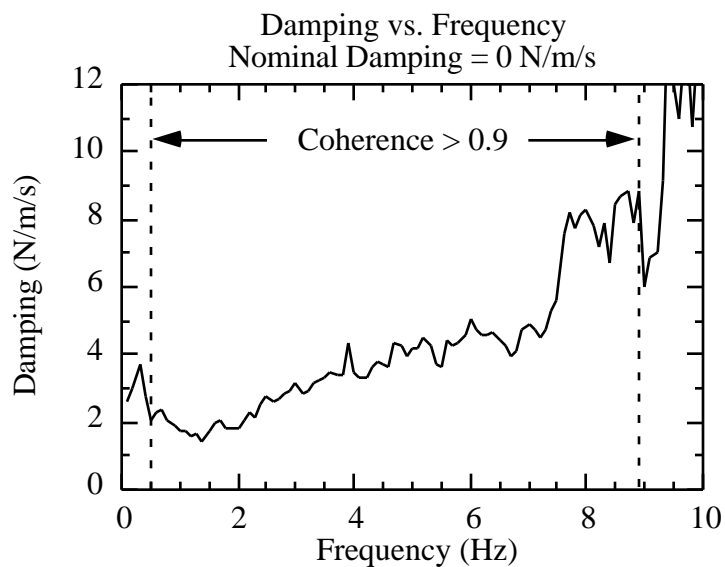


Figure 4.8 Estimated handle damping as a function of frequency for the null environment simulation. The estimate was only valid in the frequency range from 0.5–8.8 Hz.

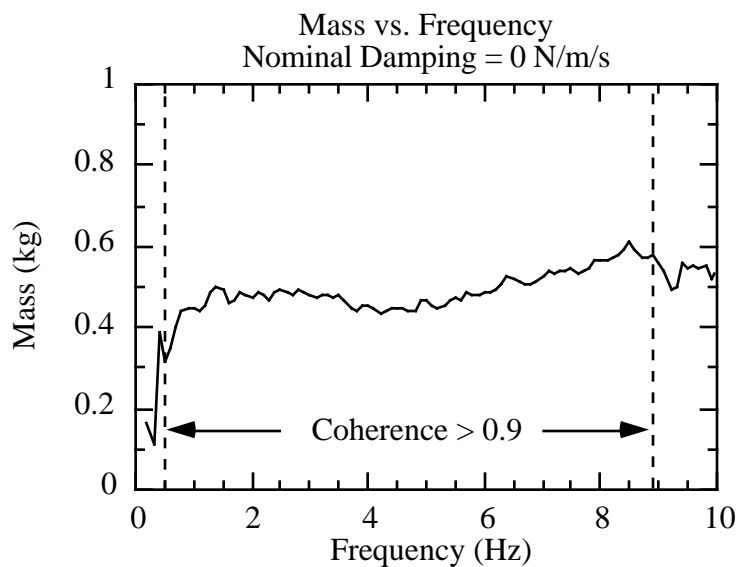


Figure 4.9 Estimated handle mass as a function of frequency for the null environment simulation. The estimate was only valid in the frequency range from 0.5–8.8 Hz.

A second set of data was collected in which the virtual damping parameter in the controller was set at 50 N·s/m. As in the null environment case, virtual mass and stiffness were nominally zero. Figures 4.10 and 4.11 are graphs of the damping and inertia vs. frequency when virtual damping was 50 N·s/m. The procedure for estimating the impedance was the same as that used for the null environment case. The estimates of damping and inertia were valid only in roughly the frequency range 0.2–8.3 Hz, where coherence was greater than 0.9.

The damping was approximately 43–49 N·s/m in the frequency range of voluntary motion, or between 86% and 98% of the nominal value. This error is consistent with the measurements of the isometric force transfer function in the frequency range from 5 to 10 Hz (i.e. force output between ~87% of commanded force). The damping measurement and the isometric force measurements provide strong evidence that in the frequency range of voluntary motion, the force output of the motor/controller is roughly 10% below nominal.

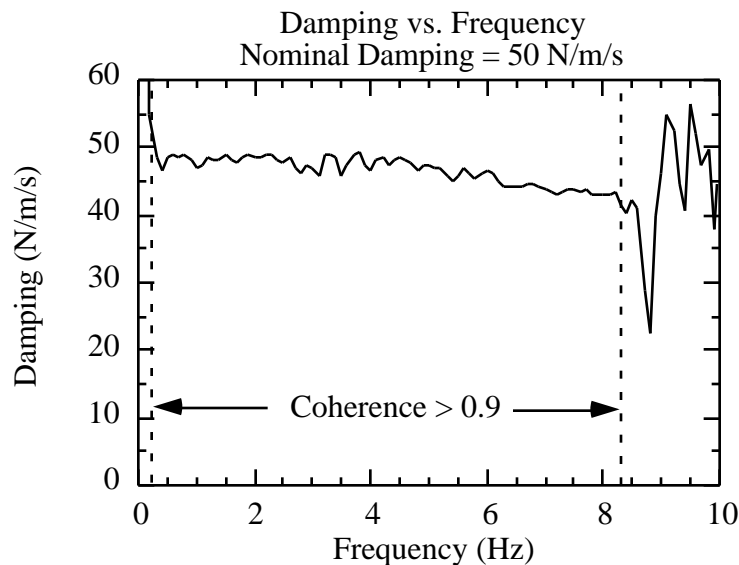
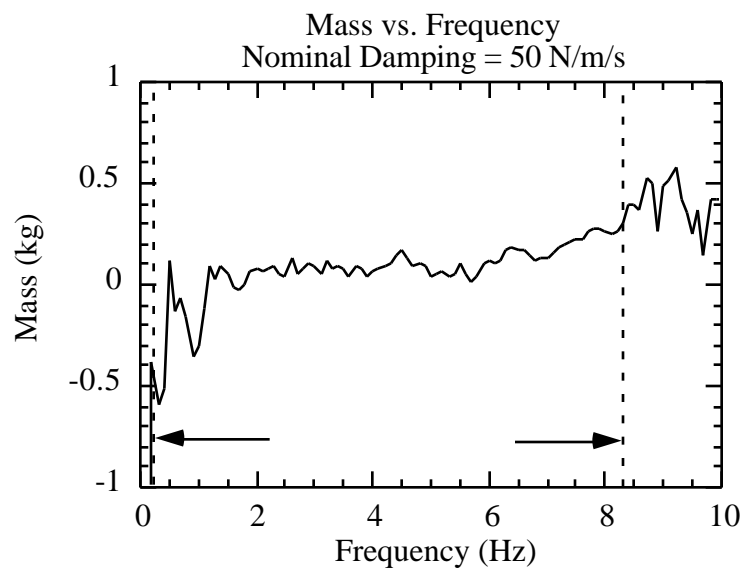


Figure 4.10 Estimated handle damping as a function of frequency for a 50 N·s/m damping simulation. The estimate was valid only in the frequency range from 0.2–8.3 Hz.



the analysis. A change of 1 ms in this estimate will shift the mass estimate by approximately 0.1 kg.

#### 4.4 Summary

The manipulandum used for the experiment has been described, and its performance quantified. The apparatus was a single degree-of-freedom, direct drive "crank", with a circular handle path of approximately 1 meter per revolution. The mechanism was controlled by a PC-based digital controller running at either 1000 or 3000 Hz. Forces up to 130 N could be generated at the handle, and handle motions as small as 1.1  $\mu\text{m}$  could be resolved. Torque output from the actuator was approximately 90% of nominal in the frequency range of voluntary human motion, and better than 80% up to 100 Hz. Output torque was a smaller fraction of commanded torque when torque amplitude was small (i.e. 2 N and less). The minimum achievable impedance of the device was approximately 4 N·s/m (damping) and 0.85 kg (inertia). Maximum achievable damping was 200 N·s/m. The apparatus was well suited for the experiments in all respects except for one: broadband noise in the motor output, which was perceptible to users.